Solar Energy 146 (2017) 389–400

Contents lists available at ScienceDirect

Solar Energy

journal homepage: www.elsevier.com/locate/solener

Comparative performance assessment of a non-ventilated and ventilated BIPV rooftop configurations in the Netherlands

M.J. Ritzen [a,b,*], Z.A.E.P. Vroon [a,c], R. Rovers [d], C.P.W. Geurts [c]

[a] Zuyd University of Applied Sciences, Nieuw Eyckholt 300, 6419 DJ Heerlen, The Netherlands
[b] Department of the Built Environment, Eindhoven University of Technology, De Wielen, 5600 MA Eindhoven, The Netherlands
[c] TNO, Stieltjesweg 1, 2628 CK Delft, The Netherlands
[d] SBS, Wollenbergstraat 37, 5581 HH Waalre, The Netherlands

ARTICLE INFO

Article history:
Received 1 September 2016
Received in revised form 20 February 2017
Accepted 21 February 2017

Keywords:
Zero energy buildings
Building envelope
Building Integrated Photovoltaics

ABSTRACT

Backside ventilation is one of the most common passive cooling methods of PV modules in the built environment, but might be under constraint when integrating PV in the building envelope. To investigate the short and long term effect of backside ventilation on Building Integrated PV (BIPV) performance and lifespan, a comparative BIPV field test is conducted in a real life lab located in the Netherlands. The field test includes 24 modules in 4 segments with different levels of backside ventilation. PV energy output, module backside temperature, relative humidity in the air gap, and air velocity in the air gap have been monitored for three years in the period January 2013–December 2015. At the end of the monitoring period Electric Luminescence (EL) images were made and Standard Testing Condition (STC) power was determined. The ventilated segments show a similar behaviour (6% difference) in PV energy output, but the non-ventilated segment shows a strong decrease of 86% in output after three years. A maximum temperature of 72 °C is reached in the ventilated segments and a maximum temperature of 83 °C in the non-ventilated segment. Relative humidity (RH) levels reach a maximum of 100% in all segments. Air velocity in the non-ventilated segment is 13–39% of the air velocity in the ventilated segments. STC power determination and EL imaging show lower peak power and more defects in the non-ventilated modules, and modules placed at vertical higher positions in the non-ventilated segment have a lower power output of 50–60%. The results indicate that, considering the first generation Metal Wrap Through (MWT) modules investigated, the non-ventilated BIPV modules exposed to the highest temperatures show the lowest power output, lowest STC power and show the most damaged cells in the EL imaging. Even though PV module manufacturing shows continuous technological advances, the methodology and results of this work has added value for the prediction of BIPV operating aspects and lifespan when designing and realizing a BIPV installation. Moreover, the BIPV field test presented in this study has been a very illustrative BIPV demonstration project for manufacturers, installers and designers.

1. Introduction

Between 1990 and 2005, global final energy consumption increased by 23%, while the associated CO_2 emissions increased by 25% (IEA, 2008). This consumption is expected to grow by another 45% between 2002 and 2025 (Ko et al., 2011). Of this global energy consumption, 20% to 40% is consumed in the built environment (Pérez-Lombard et al., 2008), of which more than 86% is based on fossil fuels (USEIA, 2011). Between 1995 and 2005, extraction of fossil fuels increased by 24% (Bruckner et al., 2012).

To lower overall energy consumption in the built environment and to lower dependency on fossil fuels, it has been agreed within the European Union (EU) that all new buildings in 2020 have to be (nearly) zero-energy buildings (*NZEB*) Pérez-Lombard et al., 2008; Frontini, 2011. *NZEB* implies that all building related operating energy is generated on the building site itself by renewable sources, calculated on a yearly basis (Torcellini et al., 2006; Agentschap, 2012).

The building envelope plays a significant role in energy performance (Ho et al., 2012), as it influences the energy gains/losses through insulation values of opaque and transparent components and also provides the necessary space for the installation of active solar energy systems for energy generation (Chynoweth, 2009).

* Corresponding author at: Zuyd University of Applied Sciences, Nieuw Eyckholt 300, 6419 DJ Heerlen, The Netherlands.
E-mail address: michiel.ritzen@zuyd.nl (M.J. Ritzen).

http://dx.doi.org/10.1016/j.solener.2017.02.042
0038-092X/

Nomenclature

AC	Alternate Current
Adc	Alternating current
BAPV	Building Added PhotoVoltaics
BIPV	Building Integrated PhotoVoltaics
CO_2	Carbon Dioxide
DC	Direct Current
DHT	Damp Heat Test
Δ_{perf}	Difference in performance
EL	Electric Luminescense
$E_{non\text{-}vent}$	Energy output of non-ventilated BIPV (AC)
EU	European Union
EVA	Ethylene Vinyl Acetate
E_{vent}	Energy output of ventilated BIPV (AC)
IEC	International Electrotechnical Commission
Imp	Power point current
IR	Infrared
Isc	Short circuit current
IV	Current voltage
kWp	kiloWatt peak, nominal power at STC of PV installations
MV	Mechanical Ventilation
MWT	Metal Wrap Through
NREL	National Renewable Energy Laboratory
NZEB	Nearly Zero Energy Building
PV	PhotoVoltaics
RH	Relative Humidity
SAM	System Advisory Model
STC	Standard Test Conditions
TCT200	Temperature Cycling Test 200
TDoT	The District of Tomorrow, field test location in the Netherlands
UK	United Kingdom
Vac	Alternating current voltage
Vdc	Direct current voltage
Vmp	Power point voltage
Voc	Open circuit voltage
Wac	Alternating current power
Wdc	Direct current power
Wp	Watt peak, nominal power at STC of PV modules

One of the solutions to provide the necessary energy in the building itself is by applying active solar energy-generating devices in the form of photovoltaic (PV) modules for electricity. In a PV system solar radiation is converted into electricity, which can be used in the building itself, stored, or can be fed into the electricity grid. As the energy received from the sun on the earth's surface in one hour is equal to approximately one year's energy needs for mankind (Mekhilef et al., 2012; Davis et al., 2001), theoretically, it is possible to fulfil our energy needs completely using the sun, even with the current efficiency of PV systems, which ranges between 12% and 19%. Moreover, within the EU, approximately 70% of the electricity consumption could be generated by PV applied on buildings, based on the current PV efficiency (Šúri et al., 2007; Defaix et al., 2012).

PV systems can be added to a building (Building Added PV - BAPV) or can be integrated in the building envelope (Building Integrated PV – BIPV), as illustrated in Fig. 1A and B. BIPV is part of the building design, possibly replacing conventional building materials such as wall cladding and/or roofing.

Integrating PV modules in the building envelope will lead to aesthetically and socially more acceptable solutions, contributing to large-scale realization of *NZEBs*. However, BIPV solutions generally result in a decrease of space between the PV installation and the thermal building envelope, negatively affecting the natural backside ventilation.

Backside ventilation is one of the methods to effectively cool PV systems (Sadineni et al., 2011; Bloem et al., 2012; Huang, 2011; Maturi et al., 2010; Petter Jelle, 2012; Tyagi et al., 2012; Gan, 2009; Wang et al., 2006; Norton et al., 2011; Gan, 2009; Mei et al., 2009), but this is under constraint when integrating PV in the building envelope. Decreasing the air gap height has a negative effect on PV performance because the efficiency of PV crystalline silicon cells drops by approximately 0.5% per °C temperature rise (Hasan et al., 2010; Quesada et al., 2012). Brinkworth and Sandberg (2006) showed in a theoretical study that minimum temperatures occurred with a roof-length-to-air-gap-width ratio of 20:1, whereas Gan et al. (2009) showed in a theoretical study that the optimal air gap width for a 35° south-orientated 3-module system in the UK was 12.5 cm, with an air velocity of approximately 0.42 m/s.

Besides lower operational performance, higher temperatures of the PV modules might lead to a shortened lifespan and lack of ventilation might lead to condensation in the building structure. This can particularly become problematic in the case of completely integrated PV without any ventilation at all (Mei et al., 2009). The Temperature Cycling Test 200 (TCT200) and Damp Heat Test

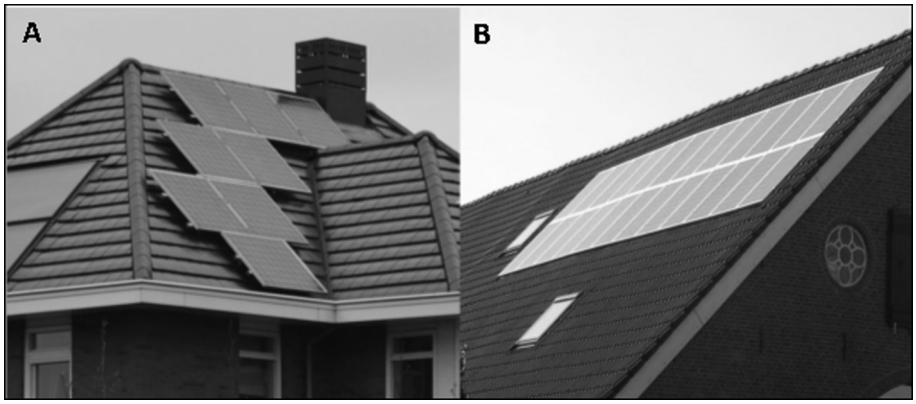

Fig. 1. Examples of two projects with (A) Building Added PV (BAPV) and (B) Building Integrated PV (BIPV) in the Netherlands.

(DHT) are the most critical tests for crystalline PV modules (Kontges et al., 2014; Rosca et al., 2012). Frequent changes in temperature in TCT200 are known to wear out the cell interconnections (Kontges et al., 2014). DHT indicates the quality of the lamination to protect the solar cells from humidity penetration. Humidity penetration causes corrosion (Ndiaye et al., 2013), which causes cell malfunctioning. The DHT proved critical for 21–13% of tested crystalline PV modules in 2009 (Kontges et al., 2014),and is perhaps the most critical for MWT modules (Rosca et al., 2012). Up to date, testing mostly takes place in lab facilities over smaller periods of time and degradation due to humidity penetration is not well known from operation in outside circumstance (Koehl et al., 2012).

PV module manufacturers guarantee, in general, a maximum decrease of 20% of the STC power over 25 years of operation (Dittmann et al., 2012), up till a temperature of 85 °C, above which the warranty is voided (Mei et al., 2009). However, research conducted in Switzerland show a decrease of 10–75% of the nominal power of the modules after a period of 12 years (Dittmann et al., 2012). According to van Kampen, et al., temperature differences between BAPV and BIPV in Europe, based on a maximum ambient temperature of 40 °C, can reach 30 °C and can exceed the 85 °C (van Kampen, 2008). In the Netherlands a non-ventilated BIPV installation shows, on average, a 15 °C higher temperature (Agentschap, 2011). Other research efforts have shown temperature difference between BAPV and BIPV of 5 °C in the Netherlands (Sinapsis et al., 2013), and 20 °C in Spain, with a lower efficiency of 7.3% (Sanchez-Friera et al., 2010).

The aim of this study is to investigate the short and long term effect of backside ventilation on BIPV performance of MWT modules.

Similar research and tests have been conducted on a smaller scale and shorter monitoring periods (Gan, 2009; Gan, 2009; Mei et al., 2009; Sinapsis et al., 2013; NREL, 2005) and similar sized arrays have been monitored, but without varying backside ventilation levels (Dittmann et al., 2012; IEC, 1998; Pacheco et al., 2012; Bahaj, 2003; De Lillo et al., 2004). Moreover, combinations of Building Integrated PV (BIPV) with other functions in the building envelope have been studied, but without the variation of ventilation (Chynoweth, 2009; Maturi et al., 2010; Sanjuan et al., 2011; Fujisawa and Tani, 1997; Ghani et al., 2012; Omer et al., 2003; Yun et al., 2007; Kaan and Reijenga, 2004).

This paper is structured as follows. In Section 2, the field test and the different methods used to simulate energy performance and measurements are presented. In Section 3, the results are outlined and Sections 4 and 5 consist of the discussion and conclusion.

2. Methodology

In this study, a 5.6 kWp BIPV rooftop field test is realized in a real life lab in the Netherlands. The field test includes 4 PV segments with different levels of backside ventilation. Each segment includes 6 modules with first generation MWT cell modules. The field test has been equipped with sensors at the top and bottom of all segments in the air gap between the PV modules and the rooftop, monitoring PV module backside surface temperatures, air velocity, and relative humidity. Moreover, the installation has been equipped to measure the output of the PV segments and the output has been simulated with the System Advisory Model (SAM) Torcellini et al., 2006. To investigate the effect of ventilation on PV performance and lifespan, the BIPV field test has been monitored for 3 years, and at the end of the monitoring period Electric Luminescence (EL) imaging and STC power determination based on current-voltage (IV) testing of all modules has been conducted. Due to project limitations, EL imaging and STC power determination were not possible before realizing the field test. A comparison is made between the ventilated and non-ventilated segments covering simulated and measured energy performance, PV module backside temperature measurements, air velocity measured in the airgap, RH levels measured in the airgap, and end of measurement evaluation of the modules in the BIPV installation. The design, realization and monitoring of the system accords with the international standard IEC 1829 (Crystalline silicon photovoltaic (PV) array – on-site measurement of IV characteristics) (IEC, 1995) and the international standard IEC 61724 (Photovoltaic system performance monitoring – guidelines for measurement, data exchange and analysis) (IEC, 1998).

2.1. Field test description

The experimental BIPV rooftop of the building "Bent to the Sun" in The District of Tomorrow (TDoT) has been developed as part of this study. TDoT is located on the European Science and Business Park Avantis in Heerlen/Aachen (on the border between the Netherlands and Germany). In TDoT four innovative and experimental buildings are being realized with increasing ambitions in the field of energy consumption and generation, material application and water consumption, including innovative BIPV solutions (indicated in Figs. 2 and 3).

The location has a moderate sea climate (type Cfb according to the Köppen Climate Classification (Kottek et al., 2006), with relatively mild summers (17.5 °C long term average), relatively mild winters (3.1 °C long term average) and annually 773 mm of precipitation (long term average) KNMI, 1981. The long term average annual temperature in Heerlen is 9.9 °C (KNMI, 1981). The long term average annual global horizontal irradiation is 1069 kWh/m^2 (Commission, 2015) and the location has a long term average of 1480 solar hours yearly (KNMI, 1981). The geographic location is 50°49′47.48″ latitude, 6°1′2.06″ longitude and 183 m altitude above mean sea level. The location is an open site without disturbance from building objects creating shadows on the field test. The highway between Heerlen (the Netherlands) and Aachen (Germany) is southwest of the location.

The field test includes 24 PV modules, which are placed in 4 segments of 6 modules each. Each segment has a different level of ventilation between rooftop and PV modules. Each module consists of 60 first generation MWT multi crystalline PV cells. MWT cells have an increased efficiency due to the electricity transport behind the cell with a conductive back sheet foil, reducing front side shadowing, in contrary to cells with the electricity transport on the front with bus bars (Mat Desa et al., 2016; Barbato et al., 2016). The lack of clearly visible bus bars possibly increases the aesthetical appearance (Figs. 4 and 5). The MWT modules consist of 4 mm ESG special front glass, EVA, and a composite film back side encapsulate (Solar, 2010), which is comparable to other mono and multi crystalline PV modules.

The difference in backside ventilation between the four segments was realized by installing the mechanical ventilation outlet behind two segments (Figs. 6-9), coupled to the building HVAC systems, with an average outlet air temperature of 17.2 °C. One segment was left as-is with a natural ventilation duct of 13 cm (Fig. 10), whereas the theoretical optimum air gap for this inclination is approximately 12.5 cm (Gan, 2009), and the air gap behind one segment was sealed, as indicated in Figs. 6 and 8. Table 1 and 2 indicate the technical aspects of the BIPV field test.

2.2. Monitoring installation

The 5.6 kWp BIPV system was installed in September 2011 and began its operation in December 2012. The applied first generation MWT cells and PV modules were produced in 2010. In December

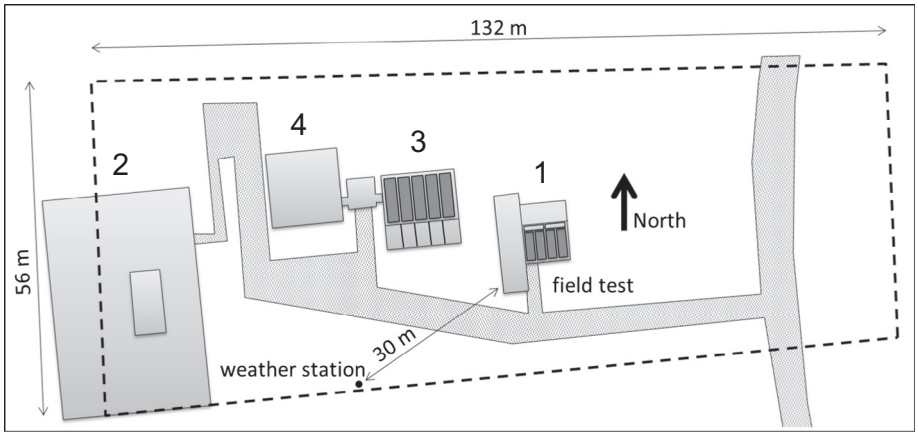

Fig. 2. Plan of The District of Tomorrow (TDoT) with four innovative building objects and field test 1.

Fig. 3. Picture of The District of Tomorrow (TDoT) with three realized innovative building objects, with at the right field test 1.

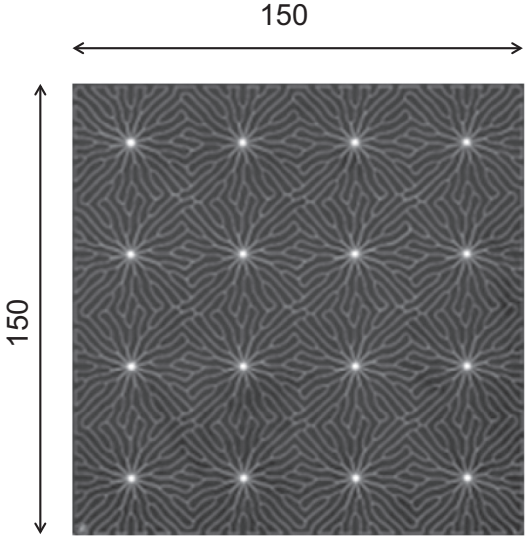

Fig. 4. Metal Wrap Through (MWT) PV cell under investigation in this study (sizes in mm).

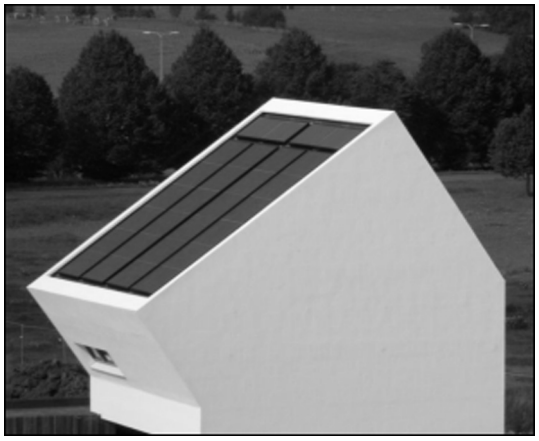

Fig. 5. Photograph of the BIPV field test in TDoT consisting of 4 portrait BIPV segments and 2 landscape solar thermal collectors at the top.

2012, all monitoring equipment was installed and was connected to a web-based data logging system in May 2013. The air-, surface-, and solar irradiance monitoring installation generate data output every 10 s, based on measurements every 1 s. The data is collected through a data logger, and sent to a FTP server, where the information is stored in .csv files. The energy performance monitoring installation generates data output with a 5-min resolution based on measurements every 1 s. The programs MS Access, MS excel, and MAT lab were applied to generate insight into the data collection presented in this research. The performance of the installation is monitored continuously since May 2013.

The monitoring installation, indicated in Figs. 8, 9, 11 and 12, consists of the following:

- 8 PT100 4-wire surface temperature sensors, type Delta Ohm TP878.1SS, placed in the centre on the back of the PV modules at the top and bottom of the segments (see Figs. 8, 9, and 11). Range +4 °C to +85 °C. Indicated by 'PTxx' in Fig. 11.
- 6 air-velocity and relative humidity sensors, type Delta Ohm HD29.371, placed in the air gap between the PV modules and the rooftop. Air-velocity range: 0.05–1 m/s, accuracy ±0.06 m/

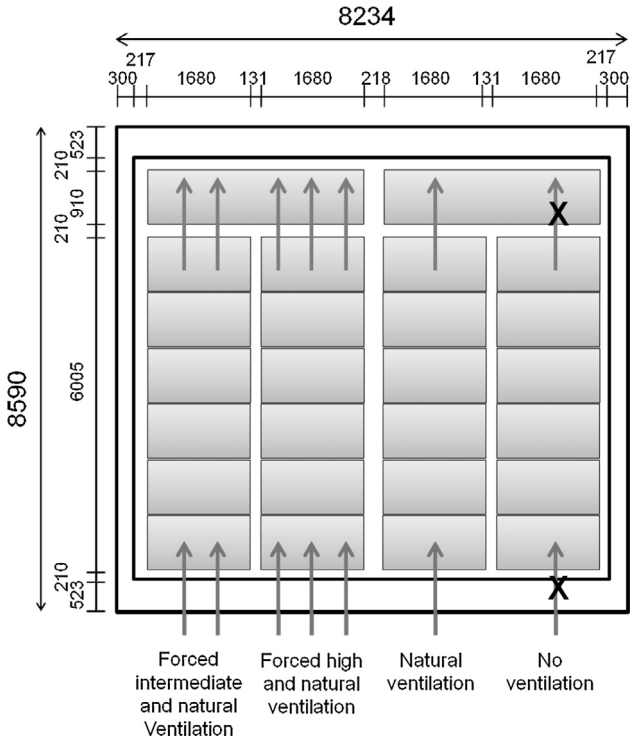

Fig. 6. Rooftop overview of the four PV segments with different levels of backside ventilation in the PV field test in TDoT (sizes in mm). Two solar thermal collectors, indicated above the four PV segments, are not included in this research.

s + 2% of measurement at 50% RH and 1013 hPa. Relative humidity range 5–98% RH, accuracy ±2.5% (5–90%RH)–±3.5% remaining range. Indicated by 'TVLxx' in Fig. 11.

- 2 relative humidity sensors, type Delta Ohm HD4817TC1.2, placed in the air gap between the PV modules and the rooftop. Relative humidity range 0–100%RH, accuracy ±2% (10–90%RH), ±2.5% outside. Indicated by 'TLxx' in Fig. 11.
- Horizontal solar irradiance is derived from a second class pyranometer (weather station type Delta Ohm HD52.3D 147R), thermopile, 0–2000 W/m^2 range, 1 W/m^2 resolution, installed at a height of approximately 191 m. above sea level, 16 m above local level, located approximately 30 m. west to south-west of the field test. (Figs. 2 and 3).
- Outside air temperature is derived from a PT100 (weather station type Delta Ohm HD52.3D 147R), range −40 °C to 60 °C, 0.1 °C resolution, with an accuracy of ±0.15 °C ± 0.1% of the measurement, installed at a height of approximately 191 m. above sea level, 16 m above local level, located approximately 30 m. west to south-west of the field test. (Figs. 2 and 3).
- The energy performance monitoring installation consists of 1 SMA sunnyboy 1200 inverter per segment, connected to a SMA sunny webbox. Generated data includes AC output (kWh) and DC and AC power (W). Note: The inverters affect the measurements and moreover, decreasing efficiency of the inverters might be of influence on the measurements (Vignola et al.).

2.3. Energy performance simulation

The energy performance of the BIPV installation was simulated with the System Advisor Model (SAM), developed by the United States National Renewable Energy Laboratory (NREL) NREL, 2014a. SAM was used to make a performance prediction for the grid-connected installation. SAM offers the possibility to select the appropriate meteorological data for the location, the appropriate PV installation specifications and offers different integration levels affecting backside ventilation, and thus performance (NREL, 2014b).

The difference in performance between the ventilated and non-ventilated BIPV has been calculated by:

$$\Delta_{perf} = \frac{E_{vent} - E_{non-vent}}{E_{vent}} \times 100 \quad (1)$$

2.4. End of measurement testing of the modules

After the three year monitoring period, the rooftop BIPV installation has been dismantled. All the modules have undergone a visual inspection before, during and after dismantling based on (Kontges et al., 2014). Due to weather circumstances with too low irradiance and clouding conditions, IR imaging did not result

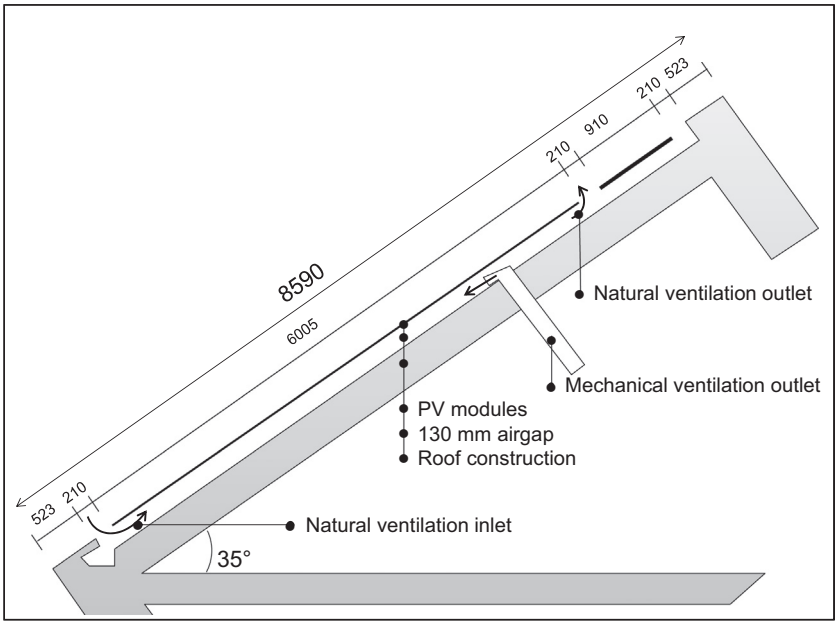

Fig. 7. Vertical section of the field test with ventilation in- and outlets providing different levels of backside ventilation (sizes in mm).

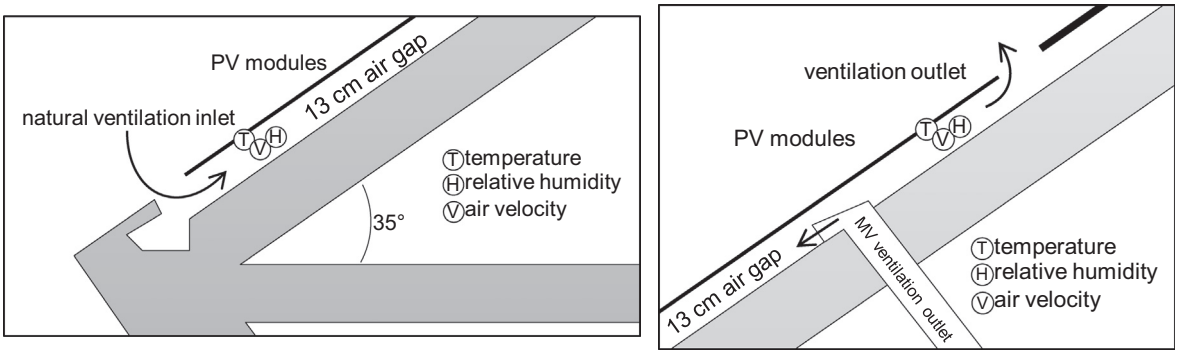

Figs. 8 and 9. Vertical sections of the bottom and top of the PV segments 1 and 2 with the locations of the sensors used in this study, the realized air gap of 13 cm for backside ventilation, and the mechanical ventilation (MV) outlet.

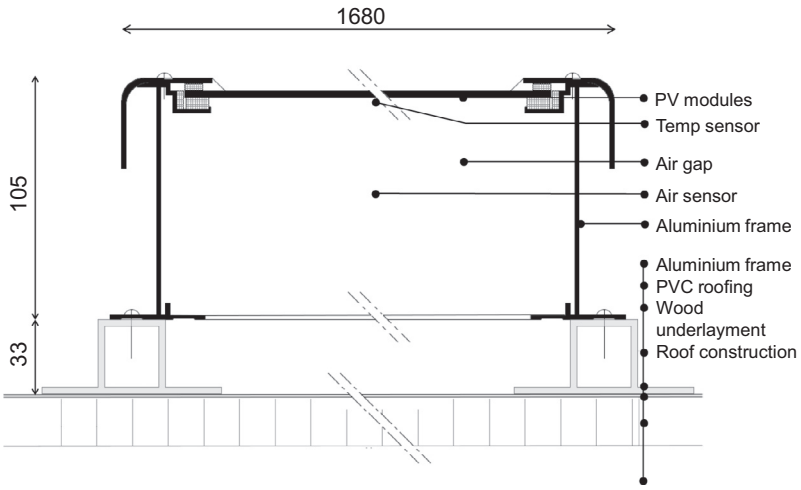

Fig. 10. Technical horizontal section of the BIPV rooftop design. In the non-ventilated segment, the top and bottom opening has been sealed. All sizes in mm.

Table 1
Technical specifications of the PV module installation at STC[1] used in SAM to calculate PV performance.

24 frameless glass-EVA-back sheet PV modules, area 1.59 m^2
4 vertical segments (6.0 × 1.68 m)
6 PV modules per segment
Multi-crystalline silicon MWT solar cells
60 cells in series per module
Direct power 234.99 W (Wdc) per module
Efficiency 14.78% per module
Nominal operating cell temperature 45 °C per module
Maximum power point voltage (Vmp) 30.05 V per module
Maximum power point current (Imp) 7.82 A per module
Open circuit voltage (Voc) 36.97 V per module
Short circuit voltage (Isc) 8.44 A per module
Temperature coefficient of Voc −0.33%/°C per module
Temperature coefficient of Isc 0.067%/°C per module
Temperature coefficient of maximum power point −0.43%/°C per module
Total installed power 5640 Wdc

[1] STC, standard test condition (cell temperature = 25°C; solar irradiance = 1 kW/m^2 and air mass = 1.5).

in useful results. A mobile lab has been used for Electric Luminescence (EL) imaging and STC power determination based on current-voltage (IV) testing at the end of the monitoring period on site. Due to project limitations, EL imaging and STC power determination on site before field test realization was not possible. EL imaging is a useful solar cell and module investigation method because it is fast, non-destructive and sensitive for non-visual defects (Crozier et al., 2011; Veldman et al., 2011), but methods to analyze EL images are still to be fully developed. Consequently, a visual count of affected cells has been conducted. The specifications of the mobile lab are the following (Tester, 2015):

Power measurement data:

- Flasher technology: long pulse LED flasher
- Luminous power: 850–1100 W/m^2
- Light colour: warm white (2000–3000 K)
- Light spectrum: (400–800 nm)
- Local inhomogeneity: <±2%
- Lighting instability: <±2%
- Repeating accuracy:<0.5% deviation
- Deviation current/voltage measurement: current:<±0.1%; voltage <±0.1%
- Accuracy: 5%

Electroluminescence data:

- Camera: cooled NIR CCD cameras
- Maximum current feed: up to 240 V/20 A
- Image resolution (total)/pixel size: ± 20 M pixels /±300 μm
- Image acquisition time:<20 s

3. Results

In this section, the performance data of the installation is presented of the three measurement years. This chapter consists of

Table 2
Technical specifications per inverter used in SAM to calculate PV performance.

Maximum AC output power 1200 Wac
Manufacturer efficiency 90.0%
Maximum DC input power 1320.13 Wdc
Nominal AC voltage 240 Vac
Maximum DC voltage 400 Vdc
Maximum DC current 12.6 Adc
Minimum MPPT DC voltage 100 Vdc
Nominal DC voltage 120 Vdc
Maximum MPPT DC voltage 320 Vdc
Power consumption during operation 0 Wdc
Power consumption at night 0.1 Wac

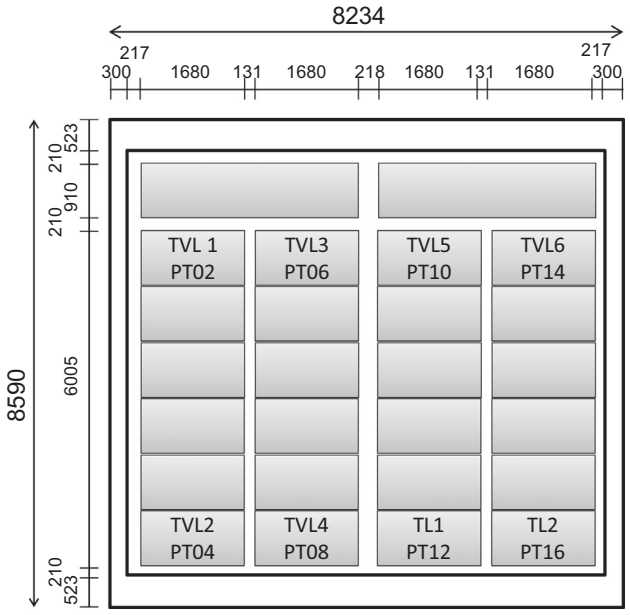

Fig. 11. Overview of the monitoring sensors on the PV segments in the field test. Abbreviations of sensors: TVL = air temperature, air velocity and relative humidity, PT = surface temperature, TL = air temperature and relative humidity.

the simulated output, measured output, condition measurements, and end-of-measurement evaluation of the PV modules.

3.1. Energy performance simulation

The energy performance of a 1.4 kWp segment reaches 1216 kWh annually in the non-ventilated situation and 1249 kWh annually in the ventilated situation on the field test location, as indicated in Table 3. The PV performance of a ventilated and a non-ventilated BIPV roof shows a difference of 2.7% on a yearly basis on the same location as the realized field test.

Table 3 indicates the lower PV performance of the non-ventilated BIPV segment compared to the ventilated BIPV segment due to the negative effect of higher operating temperatures on the performance. Moreover, this small difference increases in warmer months.

3.2. Energy performance measurements

The energy output is 1179 kWh for the double mechanical ventilated segment and 1006 kWh for the non-ventilated segment annually in the first year, 1210 kWh for the double mechanical ventilated segment and 535 kWh for the non-ventilated segment in the second year and 1112 kWh for the double mechanical ventilated segment and 160 kWh for the non-ventilated segment in the third year, as indicated in Table 4. The measured difference between the naturally ventilated segment and the non-ventilated segment is 15% in the first year and increases to 82% in the third year, as indicated on a monthly basis in Fig. 13.

Figs. 13 and 14 indicate the difference between the measured output of the different segments. Moreover, the non-ventilated segment 4 shows a significant decrease of performance and the mechanical ventilated segments show a significant increase in performance, indicating a possible correlation between ventilation and lifespan of PV modules, without taking into account possible effects related to the inverter technology applied.

3.3. PV module backside temperature, air velocity, and RH measurements

Over the monitoring period, the 10 s average maximum daily temperatures measured at the back side of the PV modules occur at the top module in the non-ventilated segment 4. Temperatures above 80 °C are measured in this segment with outside temperatures between 30 °C and 36 °C, while the daily amplitudes are over 66 °C in this segment, as indicated in Figs. 15 and 16. Previous research efforts have shown temperatures of 65 °C (France and Germany, ventilated BIPV roof) (Dittmann et al., 2012; Guiot et al., 2012), 70 °C (Singapore, ventilated BIPV roof) (Wittkopf et al., 2012), 72 °C (the Netherlands, non-ventilated BIPV roof) (Sinapsis et al., 2013; Guiot et al., 2012), 80 °C (Italy and Spain, non-ventilated) (Sanchez-Friera et al., 2010; Chatzipanagi et al., 2012) and 85 °C (Switzerland, non-ventilated) (van Kampen, 2008). Moreover, in the non-ventilated segment, the lowest temperatures go down to −8 °C.

Over the monitoring period, the daily measured maximum relative humidity at the top of the segments shows in the mechanical ventilated segments and the non-ventilated segment 100%RH, indicating a risk of condensation, indicated in Fig. 16. Due to sensor failure, there is no reliable data of segment 3. Moreover, Fig. 17 indicates the larger bandwidth of RH levels in the non-ventilated segment.

Over the monitoring period the average air velocity in the air gap between the PV modules and the roof top was 0.04 m/s in the non-ventilated segment, 0.11 m/s in the natural ventilated segment, 0.16 m/s for the single mechanical ventilated segment, and 0.34 m/s for the double mechanical ventilated segment.

3.4. End of measurement testing of the modules

Before, during and after dismantling, none of the modules showed deterioration visually. One module was severely damaged during handling, and STC power determination and EL imaging was therefore not possible. STC power determination of the remaining modules showed a decrease between 7% in the forced ventilated segments and 60% in the non-ventilated segment, indicated in Table 5 and Fig. 18, which show the STC power (Wp) per module after the monitoring period (compared to STC initial power of 230 Wp). Comparable failures were detected in a Swiss investigation after a 12-year monitoring period (Dittmann et al., 2012). In EL imaging, black areas indicate disconnection and failure of (part of) cells. Number of cells affected per module, based on a visual count, range between 3 in the forced ventilated segments and 58 in the non-ventilated segment, indicated in Table 5 and Fig. 19. Due to the inverter setup based on 4 string inverters with 6 modules in series, the significant difference in STC power of the modules indicated in Table 5 and Fig. 18 influences the electrical performance.

Figs. 20 and 21 are EL images of the best (A2) and worst (D2) module of the BIPV installation. Clearly visible in these images is the difference in the number of affected cells.

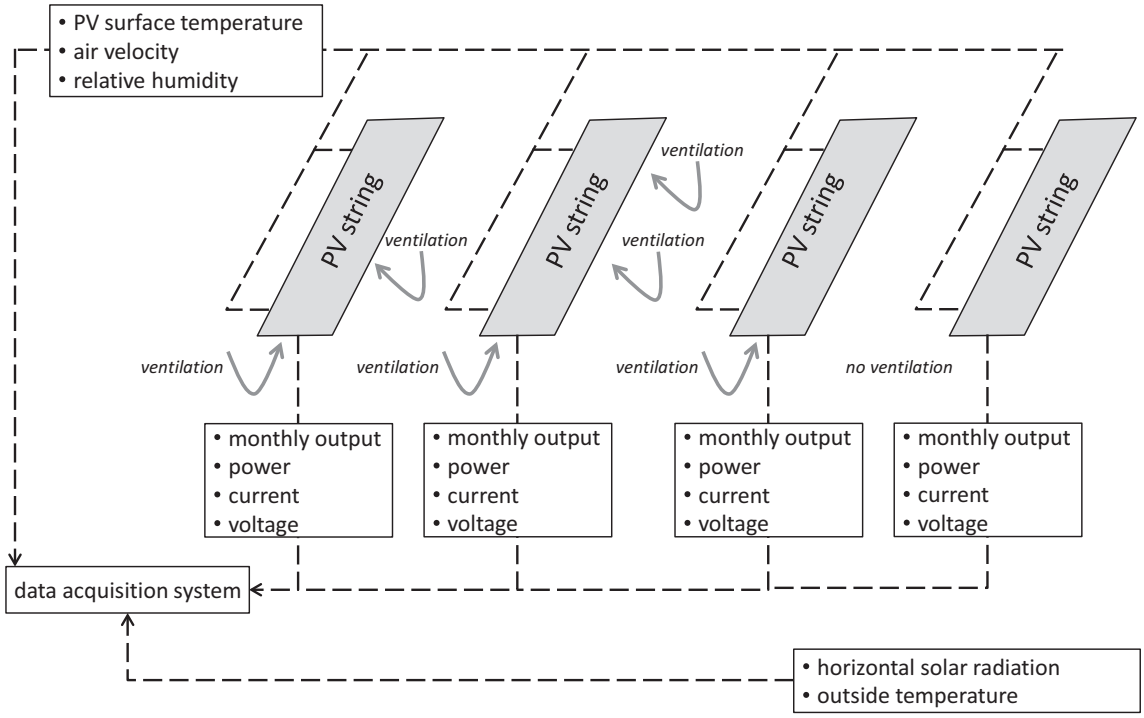

Fig. 12. Overview of monitoring in the field test consisting of condition sensors on the PV installation, PV performance, and outside conditions.

Table 3
Simulated PV output for a non-ventilated and ventilated segment on the location of the field test.

Month	Non-ventilated segment	Ventilated segment	Difference
January	36	37	1.2%
February	56	57	1.9%
March	118	121	2.6%
April	123	126	2.5%
May	152	158	4.0%
June	138	142	2.7%
July	167	173	3.3%
August	137	141	2.8%
September	114	117	2.4%
October	93	95	2.2%
November	47	48	2.5%
December	35	35	1.6%
Total	1216	1249	2.7%

4. Discussion

This paper covers the investigation of the effect of ventilation on the performance and lifespan of non-ventilated and ventilated BIPV rooftop configurations in the Netherlands.

In this study, 24 first generation MWT modules produced in 2010 have been applied in 4 different ventilation configurations and have been studied for 3 years, contributing to insight in the degradation mechanism. PV modules that are currently produced have undergone technical improvements resulting in less vulnerable MWT modules for BIPV application with less or none ventilation, and results from this study should therefore be interpreted in the context of ongoing technological development.

Performance measurements, temperature measurements, relative humidity measurements and end of monitoring EL imaging indicate failures in a non-ventilated BIPV configuration corresponding with failures observed in damp heating testing and temperature cycle testing. However, due to the limited number of modules tested and the real life circumstances repetitive testing is recommended. Moreover, measurements should be conducted in future research on module level to prevent effects such as electrical mismatch between modules and inverter control and create more insight in the temperature and relative humidity levels throughout the complete segments.

The EL imaging interpretation is based on visual counting, and this processing should undergo further refinement in order to obtain quantitative results. Moreover, EL imaging and independent STC power determination on site, directly before installation could provide important additional information.

Correlation with external meteorological conditions such as precipitation, wind velocities and wind direction are outside of the scope of this study, but outside air movement influence air velocities above the modules and in the air gap, affecting module

Table 4
Annual measured and simulated output (kWh) per segment (simulation based on 0.5% efficiency decrease per year) over the monitoring period of 3 years.

	Segment 1 (kWh) forced intermediate and natural ventilation	Segment 2 (kWh) forced high and natural ventilation	Segment 3 (kWh) natural ventilation	Segment 4 (kWh) non-ventilated)	Non-ventilated simulation (kWh)	Ventilated simulation (kWh)
2013	1177	1180	1183	1006	1216	1249
2014	1167	1210	1154	535	1209	1243
2015	1094	1112	932	160	1203	1237

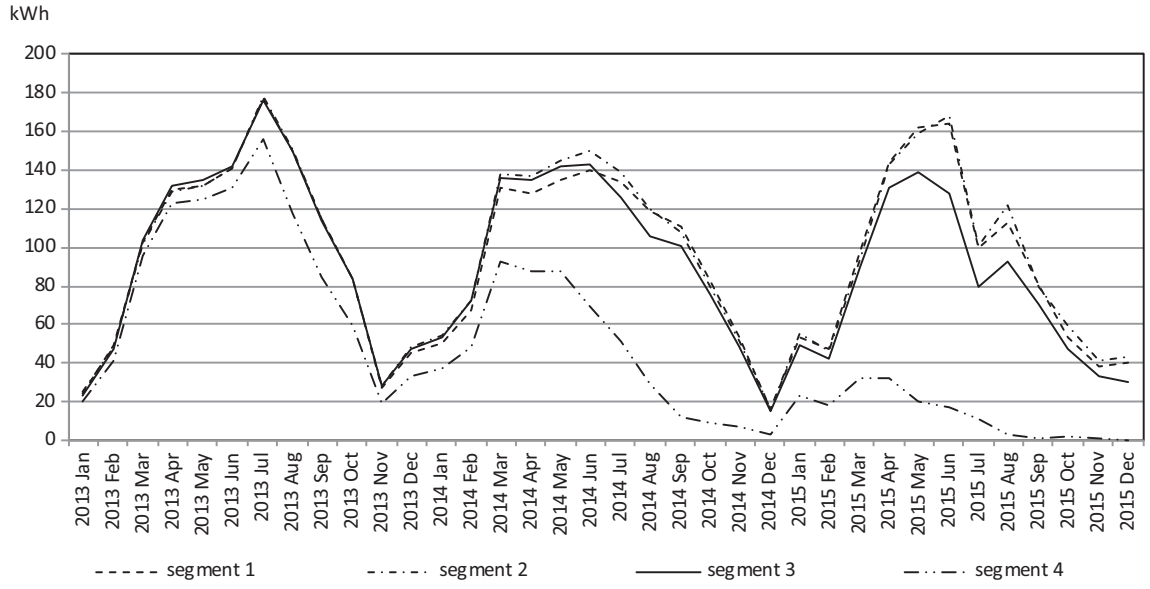

Fig. 13. Monthly measured output (kWh) for the four segments over the monitoring period of 3 years.

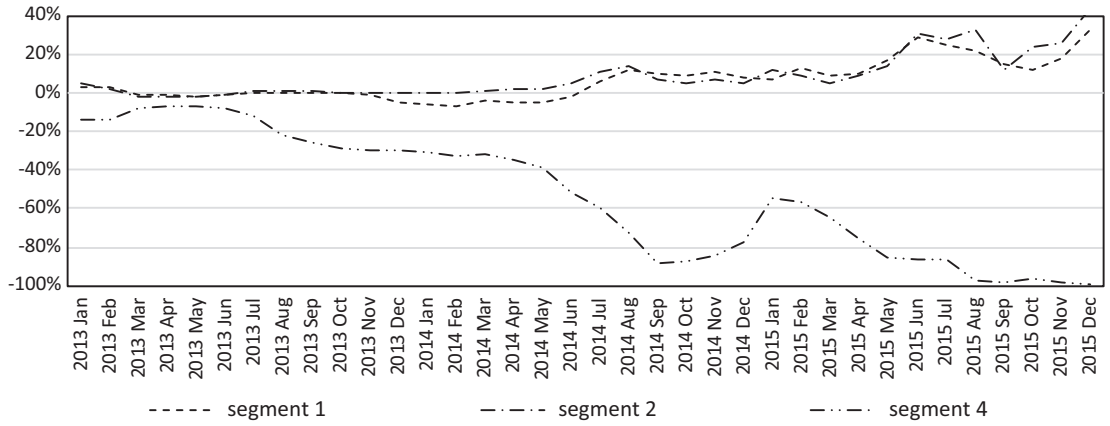

Fig. 14. Monthly relative energy output for the segments 1, 2 and 4 compared to the natural ventilated segment 3, over the monitoring period of 3 years.

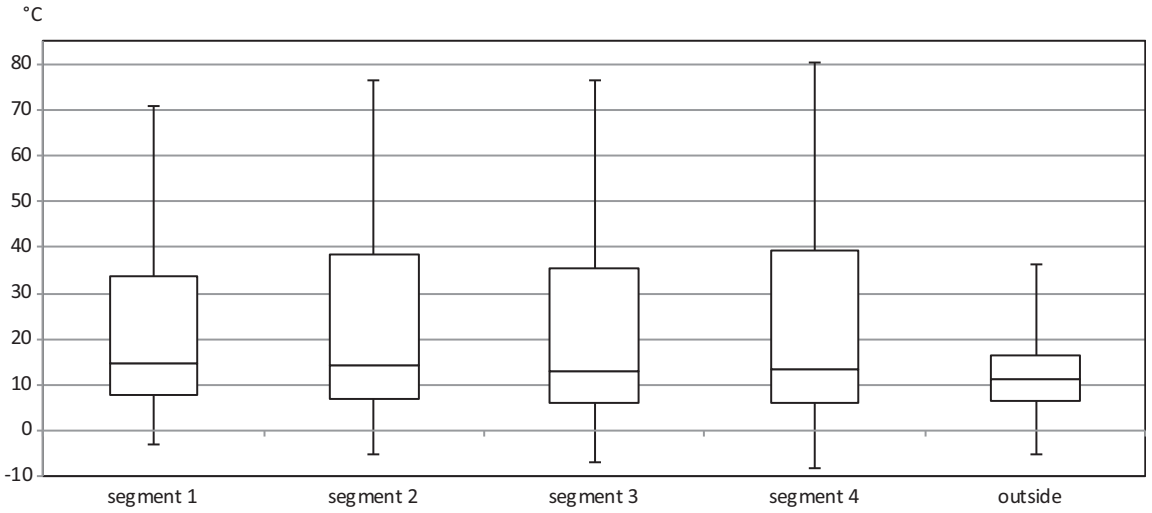

Fig. 15. Box-and-whisker plot of the daily maximum and minimum module backside surface temperatures measured at the top of the segments and the outside temperatures over the monitoring period of 3 years.

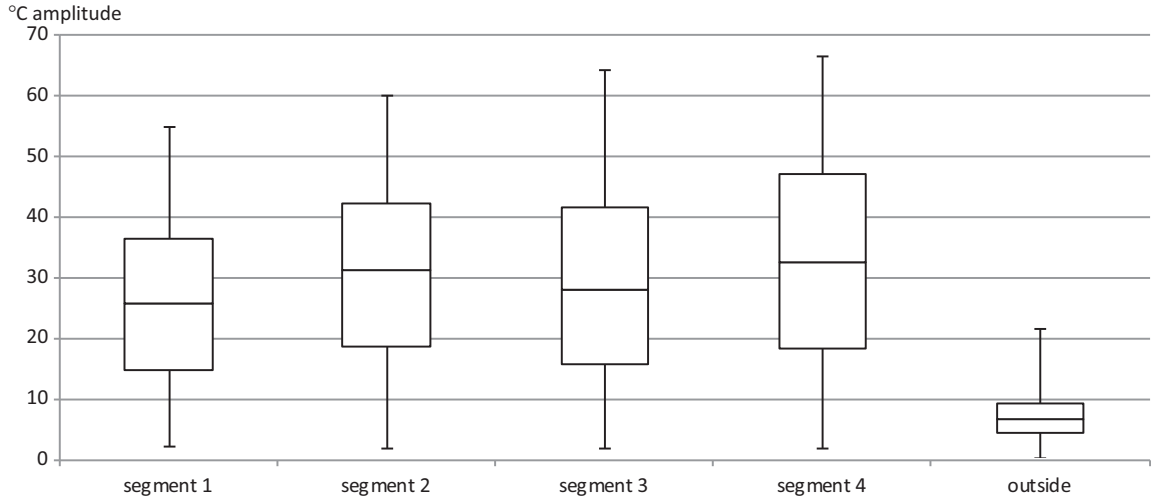

Fig. 16. Box-and-whisker plot of the daily module backside surface temperature amplitudes at the top of the segments and the outside air temperature over the monitoring period of 3 years.

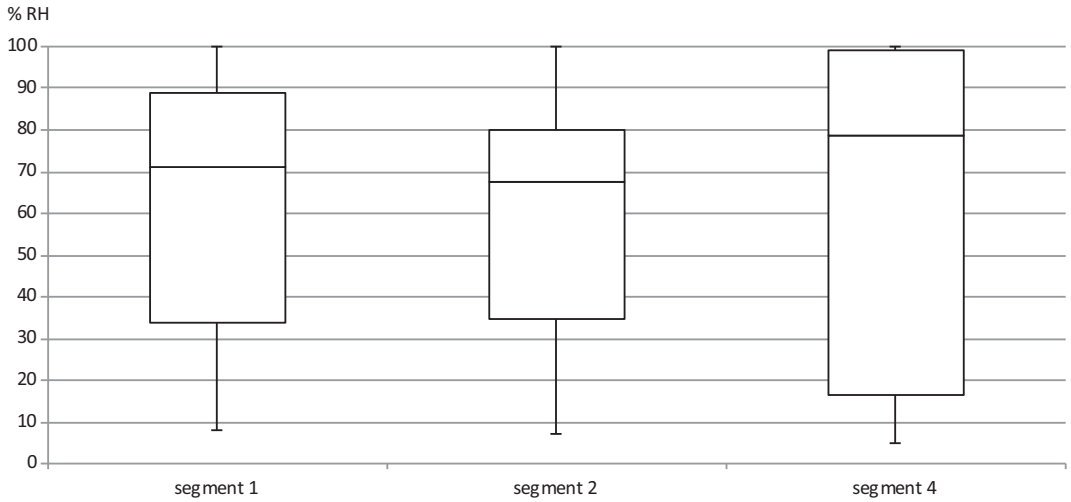

Fig. 17. Box-and-whisker plot of the daily measured maximum and minimum RH in the air gap at the top of the segments over the monitoring period of 3 years.

Table 5
STC power determination of modules, power loss and numbers of cells affected (visual count of EL imaging).

Module	Power (Wp)	Power loss (%)	Cells affected	Module	Power (Wp)	Power loss (%)	Cells affected
A1	209	9.13	6	C1	169	26.52	24
A2	213	7.39	3	C2	183	20.43	14
A3	196	14.78	13	C3	195	15.22	16
A4	170	26.09	17	C4	200	13.04	13
A5	167	27.39	23	C5	176	23.48	23
A6	198	13.91	9	C6	208	9.57	10
B1	197	14.35	6	D1	112	51.30	52
B2	213	7.39	4	D2	92	60.00	58
B3	196	14.78	8	D3	124	46.09	44
B4	139	39.57	NA	D4	160	30.43	26
B5	194	15.65	8	D5	185	19.57	14
B6	NA		NA	D6	199	13.48	11

temperature (Brinkworth and Sandberg, 2006). Moreover, precipitation affects module temperature and RH levels, while in the winter snow can influence directly the solar irradiance on the PV modules.

As BIPV modules are part of the building structure, detailing of the entrance and exit of air gaps and the BIPV support structure in the air gap has to be well designed because they affect the efficiency of the backside cooling, stressing the importance of a mul-

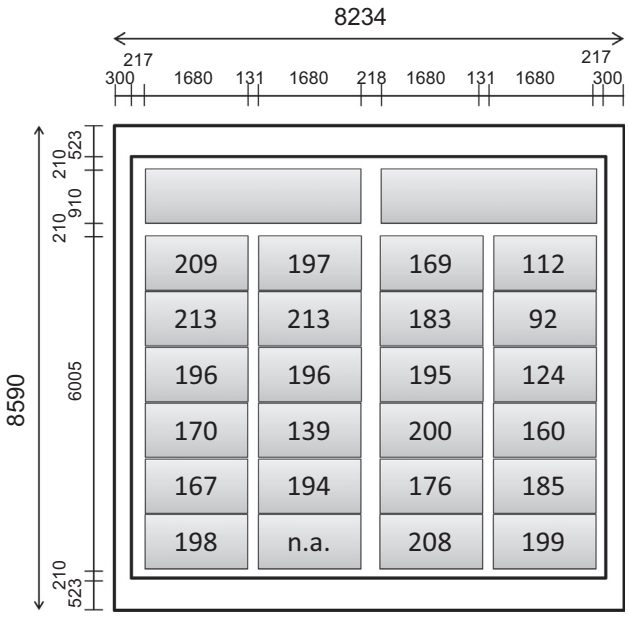

Fig. 18. Rooftop overview of the four PV segments with STC power (Wp) indicated per module.

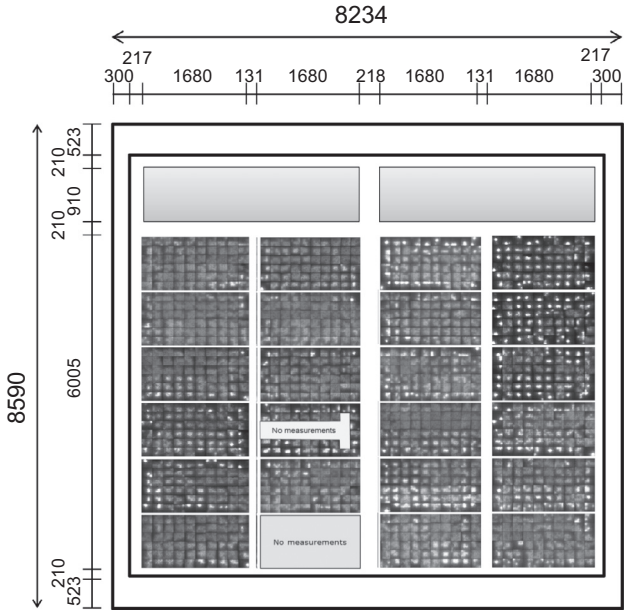

Fig. 19. Rooftop overview of the four segments with EL image per module.

tidisciplinary approach between building designers and electrical technical engineers.

5. Conclusions

In the first year of monitoring, the simulated PV output difference between a ventilated and non-ventilated configuration is 3% and the measured difference is 15%. The monitored difference increases to 82% in the third year, indicating failures in the non-ventilated configuration which increase over time.

Repetitive operating temperatures of 80 °C occurred in the non-ventilated configuration and daily temperature amplitudes reached 60 °C in the non-ventilated configuration. Moreover, in the natural ventilated and non-ventilated configuration there is a risk of condensation due to 100% relative humidity, which could lead to moisture in the building skin if PV panels would replace the roofing material. The average air velocity in the non-ventilated segment was 13% of the air velocity in the double mechanical ventilated segment. End of monitoring STC power measurement showed a decrease of 7% Wp in the forced ventilated configuration and 60% Wp in the non-ventilated configuration. EL imaging showed up to 97% cell defects in a non-ventilated module, while visual end of monitoring inspection showed no results.

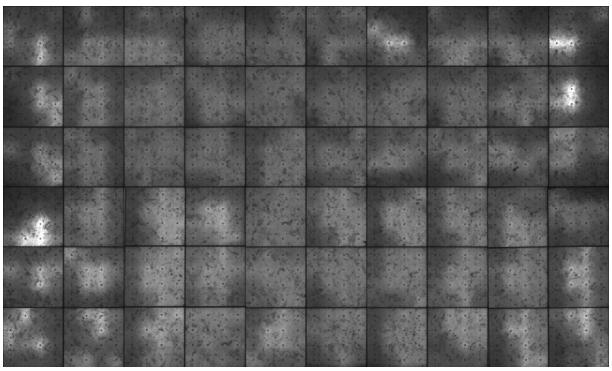

Fig. 20. EL image of mechanical ventilated module A2.

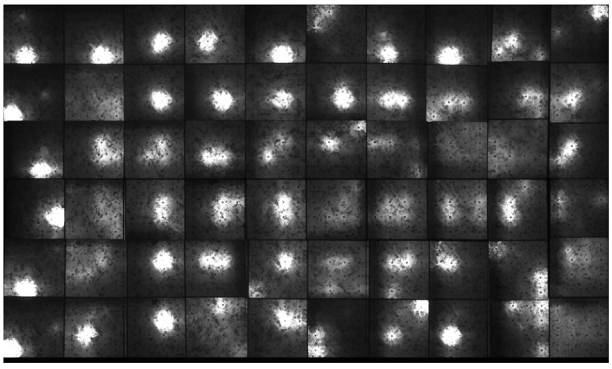

Fig. 21. EL image of non-ventilated module D2.

This study indicates a possible correlation between less ventilation, higher operating temperatures, larger daily temperature amplitudes and decreased performance of the first generation MWT PV modules under investigation (produced in 2010). Ventilation might prove to be an effective way to prevent PV modules from accumulating heat with collateral negative effects on PV output and lifespan. Results of this study should be used within the context of ongoing technological improvement of PV installations.

From a building perspective, this study indicates that combining building related mechanical ventilation outlets with PV installations proves to be an effective method to combine two installations, because in this case, the mechanical ventilation cools PV modules in the summer, heats PV modules in the winter to prevent snow accumulation and the solution prevents ducts on the rooftop that could inflict shadow on the PV modules.

This study indicates the added value of long term monitoring to support the technical improvement of PV and the acceleration of BIPV application and in future, similar studies are recommended in different climatic zones with current BIPV components to investigate the effect of ventilation on BIPV performance.

Acknowledgement

This research was partially funded by the Dutch Organization for Scientific Research (NWO), project number 023.001.198, and

by the Foundation Innovation Alliance (SIA), project number PRO-2-015 IMDEP. The author would like to thank all participants of these projects as well as the colleagues at Zuyd; George Vervuurt†, Alex Masolin, Sander van Heumen and Marc Dirix for supporting this study.

References

Agentschap, N.L., 2011. Gebouwintegratie zonnestroomsystemen. Praktijkvoorbeelden van succesvolle producten.

Agentschap, N.L., 2012. Nationaal Plan voor het bevorderen van bijna-energieneutrale gebouwen in Nederland.

Bahaj, A.S., 2003. Photovoltaic roofing: issues of design and integration into buildings. Renew. Energy 28 (14), 2195–2204.

Barbato, M. et al., 2016. Reverse bias degradation of metal wrap through silicon solar cells. Sol. Energy Mater. Sol. Cells 147, 288–294.

Bloem, J.J. et al., 2012. An outdoor test reference environment for double skin applications of building integrated photovoltaic systems. Energy Build. 50, 63–73.

Brinkworth, B.J., Sandberg, M., 2006. Design procedure for cooling ducts to minimise efficiency loss due to temperature rise in PV arrays. Sol. Energy 80 (1), 89–103.

Bruckner, M. et al., 2012. Materials embodied in international trade – Global material extraction and consumption between 1995 and 2005. Glob. Environ. Change 22 (3), 568–576.

Chatzipanagi, A., Frontini, F., Dittmann, S., 2012. Investigation of the influence of module working temperature on the performance of BIPV modules. In: 27th EU-PVSEC. 2012: Frankfurt, Germany.

Chynoweth, P., 2009. The built environment interdiscipline: a theoretical model for decision makers in research and teaching. Structural Survey [conceptual paper] 2009 [cited 27 4], 301–310].

Commission, J.R.C.E., 2015. Photovoltaic Geographical Information System (PVGIS). (cited 2015 1–10).

Crozier, J.L., van Dyk, E.E., Vorster, F.J., 2011. High Resolution Spatial Electroluminescence Imaging of Photovoltaic Modules.

Davis, M.W., dougherty, B., Fanney, A., 2001. Prediction of building integrated photovoltaic cell temperatures. J. Sol.Energy Eng. 123 (2), 200–210.

De Lillo, A., et al., 2004. Effects of BIPV on Performance. In: PV SEC. Paris, France.

Defaix, P.R. et al., 2012. Technical potential for photovoltaics on buildings in the EU-27. Sol. Energy 86 (9), 2644–2653.

Dittmann, S., et al., 2012. Module characterisation of a roof integrated PV system after a 12-year operation period in the Swiss midlands, in 31st EU-PVSEC. Frankfurt.

Frontini, F., 2011. Daylight and solar control in building: a new angle selective see-thorough PV-facade for solar control. In: PLEA 2011.

Fujisawa, T., Tani, T., 1997. Annual exergy evaluation on photovoltaic-thermal hybrid collector. Sol. Energy Mater. Sol. Cells 47 (1–4), 135–148.

Gan, G., 2009. Numerical determination of adequate air gaps for building-integrated photovoltaics. Sol. Energy 83 (8), 1253–1273.

Gan, G., 2009. Effect of air gap on the performance of building-integrated photovoltaics. Energy 34 (7), 913–921.

Ghani, F., Duke, M., Carson, J.K., 2012. Effect of flow distribution on the photovoltaic performance of a building integrated photovoltaic/thermal (BIPV/T) collector. Sol. Energy 86 (5), 1518–1530.

Guiot, T., et al., 2012. Thermal Behaviour of Rooftop BIPV Systems: An Experimental Approach. In: 27th EU-PVSEC. 2012: Frankfurt, Germany.

Hasan, A. et al., 2010. Evaluation of phase change materials for thermal regulation enhancement of building integrated photovoltaics. Sol. Energy 84 (9), 1601–1612.

Ho, C.J., Tanuwijava, A.O., Lai, C.-M., 2012. Thermal and electrical performance of a BIPV integrated with a microencapsulated phase change material layer. Energy Build. 50, 331–338.

Huang, M.J., 2011. Two phase change materials with different closed shape fins in building integrated photovoltaic system temperature regulation. In: World Renewable Energy Congress 2011, Linkoping, Sweden.

IEA, 2008. I.E.A., Worldwide Trends in Energy Use and Efficiency.

IEC, 1995. I.e.c., IEC 1829 Chrystalline Silicon Photovoltaic (PV) Array – On-site Measurement of I–V Characteristics.

IEC, 1998. I.E.C., IEC 61724 International Standard Photovoltaic System Performance Monitoring – Guidelines for Measurement, Data Exchange and Analysis. IEC.

Kaan, H., Reijenga, T., 2004. Photovoltaics in an architectural context. Prog. Photovoltaics Res. Appl. 12, 395–408.

KNMI, 2013. *Maastricht, langjarig gemiddelden, tijdvak 1981–2010*. Available from: <http://www.klimaatatlas.nl/tabel/stationsdata/klimtab_8110_380.pdf>.

Ko, J., Widder, L., 2011. Building envelope assessment tool for system integrated design. In: PLEA 2011. Louvain-la-Neuve, Belgium.

Koehl, M., Heck, M., Wiesmeier, S., 2012. Modelling of conditions for accelerated lifetime testing of Humidity impact on PV-modules based on monitoring of climatic data. Sol. Energy Mater. Sol. Cells 99, 282–291.

Kontges, M. et al., 2014. Review of Failures of Photovoltaic Modules – Report IEA-PVPS T13-01:2014, PVPS, Editor.

Kottek, M. et al., 2006. World Map of the Köppen-Geiger climate classification updated. Meteorol. Z. 15 (3), 259–263.

Mat Desa, M.K. et al., 2016. Silicon back contact solar cell configuration: A pathway towards higher efficiency. Renew. Sustain. Energy Rev. 60, 1516–1532.

Maturi, L. et al., 2010. Analysis and monitoring results of a BIPV system in northern Italy. In: PVSEC. Valencia, Spain.

Mei, L. et al., 2009. Equilibrium thermal characteristics of a building integrated photovoltaic tiled roof. Sol. Energy 83 (10), 1893–1901.

Mekhilef, S., Saidur, R., Kamalisarvestani, M., 2012. Effect of dust, humidity and air velocity on efficiency of photovoltaic cells. Renew. Sustain. Energy Rev. 16 (5), 2920–2925.

Ndiaye, A. et al., 2013. Degradations of silicon photovoltaic modules: A literature review. Sol. Energy 96, 140–151.

Norton, B. et al., 2011. Enhancing the performance of building integrated photovoltaics. Sol. Energy 85 (8), 1629–1664.

NREL, 2005. N.R.E.L., Procedure for Measuring and Reporting the Performance of Photovoltaic Systems in Buildings.

NREL, 2014. N.R.E.L. SAM homepage. Available from: <https://sam.nrel.gov/> (cited 2014 15-12-2014).

NREL, 2014. N.R.E.L. SAM. PV System Advisory Model. Available from: <https://sam.nrel.gov/>.

Omer, S.A., Wilson, R., Riffat, S.B., 2003. Monitoring results of two examples of building integrated PV (BIPV) systems in the UK. Renew. Energy 28 (9), 1387–1399.

Pacheco, R., Ordóñez, J., Martínez, G., 2012. Energy efficient design of building: A review. Renew. Sustain. Energy Rev. 16 (6), 3559–3573.

Pérez-Lombard, L., Ortiz, J., Pout, C., 2008. A review on buildings energy consumption information. Energy Build. 40 (3), 394–398.

Petter Jelle, B., Breivik, C., Drolsum Røkenes, H., 2012. Building integrated photovoltaic products: a state-of-the-art review and future research opportunities. Sol. Energy Mater. Sol. Cells 100, 69–96.

Quesada, G. et al., 2012. A comprehensive review of solar facades. Opaque solar facades. Renew. Sustain. Energy Rev. 16 (5), 2820–2832.

Rosca, V., Bennet, I.J., Eerenstein, W.E., 2012. Systematic reliability studies of back-contact photovoltaic modules. In: SPIE Optics and Photonics Conference. San Diego, USA.

Sadineni, S.B., Madala, S., Boehm, R.F., 2011. Passive building energy savings: a review of building envelope components. Renew. Sustain. Energy Rev. 15 (8), 3617–3631.

Sanchez-Friera, P. et al., 2010. Influence of design parameters on the nominal operation cell temperature of pv modules. In: EU-PVSEC, Valencia, Spain.

Sanjuan, C. et al., 2011. Energy performance of an open-joint ventilated façade compared with a conventional sealed cavity façade. Sol. Energy 85 (9), 1851–1863.

Sinapsis, K., et al., 2013. The glass-glass aesthetic energy roof: thermal behavior for various ventilation levels. In: 28th EU PVSEC. Paris.

Solar, S., Product Data Sheet; 2010.

Šúri, M. et al., 2007. Potential of solar electricity generation in the European Union member states and candidate countries. Sol. Energy 81 (10), 1295–1305.

Tester, S., 2015. Mobile Quality Inspection for Photovoltaic Panels.

Torcellini, P. et al., 2006. Zero Energy Buildings: A Critical Look at the Definition, in ACEEE Summer Study. NREL, California.

Tyagi, V.V., Kaushik, S.C., Tyagi, S.K., 2012. Advancement in solar photovoltaic/thermal (PV/T) hybrid collector technology. Renew. Sustain. Energy Rev. 16 (3), 1383–1398.

USEIA, 2011. U.S.E.I.A., International Energy Outlook 2011. U.S. Energy Information Administration.

van Kampen, B., 2008. Actual Temperatures of Building Integrated PV Modules, Study in the Framework of the EU IP Performance Project.

Veldman, D., et al., 2011. Non-destructive testing of crystalline silicon photovoltaic back-contact modules. In: Photovoltaic Specialists Conference (PVSC), 2011 37th IEEE.

Vignola, F., Mavromatakis, F., Krumsick, J. Performance of PV inverters.

Wang, Y. et al., 2006. Influence of a building's integrated-photovoltaics on heating and cooling loads. Appl. Energy 83 (9), 989–1003.

Wittkopf, S. et al., 2012. Analytical performance monitoring of a 142.5 kWp grid-connected rooftop BIPV system in Singapore. Renewable Energy 47, 9–20.

Yun, G.Y., McEvoy, M., Steemers, K., 2007. Design and overall energy performance of a ventilated photovoltaic façade. Sol. Energy 81 (3), 383–394.